Quantifying the Effects of Hindcast Surface Winds and Ocean Currents on Oil Spill Contact Probability in the Gulf of Mexico

Zhen Li and Walter Johnson
Division of Environmental Sciences, Bureau of Ocean Energy Management
45600 Woodland Road, Sterling, VA 20166
zhen.li@boem.gov

***Abstract*—The U.S. Department of the Interior, Bureau of Ocean Energy Management conducts an oil spill risk analysis (OSRA) prior to oil and gas leasing, exploration, or development on the U.S. Outer Continental Shelf. The OSRA model uses hindcast surface winds and ocean currents to calculate hundreds of thousands of trajectories initiated from hypothetical oil spill locations and estimates contact probability of these trajectories with resources that are of biological, social and economic importance. Here, the map distributions of potential oil spill contact probability to entire waters in the Gulf of Mexico are generated every day from day 1 to day 30 using 6-hourly surface winds and 3-hourly ocean currents from time periods of 1993–1998 and 2000–2006. Results show that strong seasonal and annual variability exists in the contact probability estimates for these two time periods, and the effects of hindcast surface winds and ocean currents on the contact probability can be quantified.**

Keywords—oil spill trajectory model; oil spill contact probability analysis; oil spill risk analysis; oil spill model

I. INTRODUCTION

Offshore oil and gas production has grown substantially with the advance in technology over the past century. Today the U.S. Outer Continental Shelf (OCS) remains a significant source of oil and gas for the nation's energy needs. As of March 2016, the OCS leased areas (about 26 million acres) produce 16 percent of domestic oil and 5 percent of domestic gas. Under the Outer Continental Shelf Lands Act, the U.S. Department of the Interior (USDOI) has the jurisdiction over the offshore OCS lands (generally 3 miles from shore) and can issue the leases for oil and gas development. The Bureau of Ocean Energy Management (BOEM), an agency in the US DOI, conducts environmental analyses under the National Environmental Policy Act prior to any offshore oil and gas lease sales. One of the primary issues addressed in BOEM's environmental documents is the probability of potential oil spill contacting environmental sensitive areas or those with commercial or recreational value.

The oil spill risk analysis (OSRA) is conducted by BOEM scientists to estimate the likelihood and timing of contact between hypothetical spills from prospective oil and gas development and environmental resources such as shoreline, marine habitats, recreational areas and other areas of biological, social and economic importance [1-4]. The OSRA model consists of three components: 1) the probability of large oil spill occurrence (defined as greater than or equal to 1,000 barrels); 2) the probability of contact to environmental resources from hypothetical oil spill locations (Conditional Probability); and 3) the probability of one or more large oil spills occurring and contacting environmental resources (Combined Probability).

This study focuses on the second component of the OSRA model, the probability of large spills contacting environmental resources, and quantifies the effects of hindcast surface winds and ocean currents to those conditional probability estimates. The estimate of a conditional probability is based on the assumption (condition) that a large oil spill occurs at a hypothetical spill location and does not factor in the probability of a large spill occurring.

The calculation of the conditional probability begins with the construction of the oil spill trajectory. The trajectories are initiated from hypothetical spill locations distributed in areas of prospective drilling and production and along projected pipeline and tanker routes. The trajectories are initiated every day from each hypothetical spill location over a time period of available hindcast wind and ocean current data, typically exceeding 10 years. The number of the trajectories contacting the environmental resources divided by the hundreds of thousands of hypothetical trajectories launched is the conditional probability of contact from a given set of launch points to an environmental resource.

The OSRA model uses hindcast surface winds and ocean currents to calculate trajectories on an hourly basis launched from hypothetical oil spill locations. The trajectories are advected by surface currents with a 3.5% wind drifting factor at a deflecting angle ranging from 0° to 25° clockwise. The drift angle is inversely proportional to wind speed and is computed using the formula in [5]. The OSRA model only considers spills greater than or equal to 1,000 barrels because those spills would persist on the water long enough for a trajectory analysis. The trajectory is allowed to travel for a maximum of 30 days in the Gulf of Mexico (GoM), and the conditional probability is computed for three designated travel times (i.e., 3, 10, and 30 days) from a given hypothetical spill location. The estimate of the conditional probability relies on the accuracy of the reanalysis winds and model simulated ocean currents. In the past the OSRA typically uses one set of wind and ocean current data of multi-year to decades to

estimate the conditional probability, where the uncertainties in these forcing files have never been evaluated.

One of the critical inputs to the OSRA model is the environmental resource areas (ERAs), which represent concentrations of wildlife, habitat, subsistence-hunting areas, or subsurface habitats located offshore. The ERAs are in the order of hundreds and are provided by the subject matter experts at BOEM who gather the spatial and temporal information from the literature, BOEM funded projects and consultation with experts in the federal and state government, academia, industry and other stakeholders. The ERAs are digitalized and mapped to the OSRA model grid before being loaded into the model. The OSRA model tabulates the contacts from the hypothetical oil spill trajectories to each of model grid cells that comprise an ERA and sums up the number of contacts as the total contacts to this ERA. The OSRA model also accounts for seasonal vulnerability of an ERA (defined as a time period when resources are present or susceptible to damage from an oil spill) by only tabulating those contacts to the ERAs during the months that the ERAs are vulnerable. The OSRA model outputs the conditional probability of contact to ERAs in the form of tables categorized by annual and seasonal time scales and trajectory travel time intervals (i.e., 3, 10, and 30 days). Because those ERAs are pre-determined and loaded into the OSRA model as inputs, should the ERAs change, it requires a re-run of the OSRA model.

This study developed a method to map distributions of conditional probability of contacts by tracing trajectories from the hypothetical oil spill locations over the entire leasing areas in the U.S. Gulf of Mexico OCS and tabulating its contacts to each ocean grid cell in the GoM. The map distributions of conditional probability of contact are calculated each day from day 1 to day 30 instead of three fixed intervals (i.e., 3, 10 and 30 days), and are estimated for seasonality for each month from January to December.

As expected, estimated conditional probabilities are subject to uncertainties in the model-simulated surface wind and ocean currents data. Here, two sets of hindcast winds and currents, one from 1993 to 1998 and the other from 2000 to 2006, are used to compute the conditional contact probability. They are all generated by the Princeton Ocean Model, but with different reanalyses winds, model domain and resolution. The monthly climatology, multi-year mean and standard deviations of conditional probability are calculated for these two time periods from day 1 to day 30, but the analysis is focused on the conditional probability at day 30.

The paper is organized as follows. Section 2 describes the method used to calculate the conditional probability map, OSRA model domain setup, monthly climatology of hindcast surface winds and currents for two time periods: 1993–1998 and 2000–2006. Section 3 discusses the variability of conditional probability on seasonal and inter-annual time scales for these two time periods. Section 4 shows an example of using the new method to estimate the contact probability with a large, seasonally varying ERA in the GoM. Section 5 summarizes the results and discusses the implications of this method for future application to BOEM's oil spill risk analysis.

II. METHOD

The existing OSRA model tabulates the contact of hypothetical trajectories to the pre-built polygons (representing the spatial and temporal resources) that are mapped to OSRA model grid. In this study, a new method to calculate the conditional probability is developed by treating each ocean grid cell in the GoM as an environmental resource. For every ocean grid cell, the total number of contacts from each hypothetical oil spill location, also known as a "Launch Point (LP)", is archived and the conditional probability is estimated. The conditional probability to an environmental resource from a set of LPs can be generated later by adding the contacts from the number of grid cells occupied by an environmental resource at a given time interval and period of vulnerability. The conditional probability can also be displayed as a map, allowing visual and quantitative comparison of conditional probability results between different sets of winds and currents.

A. OSRA Model Domain and Launch Points

As shown in Fig. 1, the OSRA model domain extends from 98°W to 78°W and 18°N to 31°N to be large enough to allow the full development of the Florida Current. The hypothetical oil spill locations, i.e. LPs, are shown as blue dots in Fig. 1. A total of 6,044 LPs, spaced at a resolution of 0.1° latitude by 0.1° longitude, are chosen to represent the entire planning areas for the Gulf of Mexico OCS (Fig. 2). The LPs include the Western, Central and Eastern Planning Areas, though the Eastern planning Area does not have any active platforms. While there are 28,564 grid cells in the OSRA model domain, a total of 20,615 are ocean grid cells. These ocean cells are tabulated when the hypothetical spill trajectories contact them.

B. Sensitivity Studies on the Number of Launch Points

For this analysis, a trajectory is initialized every day over the time period of the hindcast winds and currents, and is computed on an hourly basis. Each year over 2.2 million trajectories are initialized from those 6,044 LPs and the contact to each of 20,615 ocean grid cell from every trajectory is tracked from day 1 to day 30. To estimate the conditional

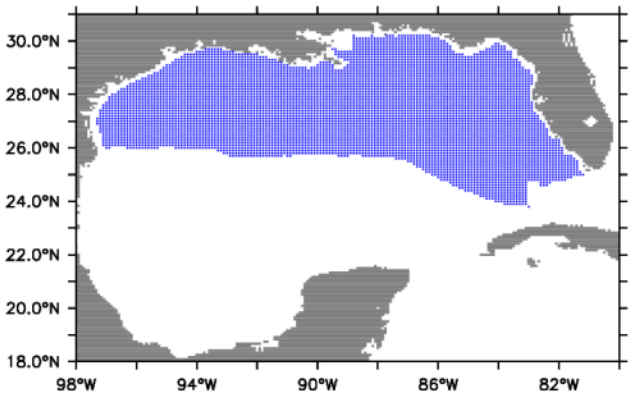

Fig. 1. OSRA model domain and hypothetical oil spill locations.

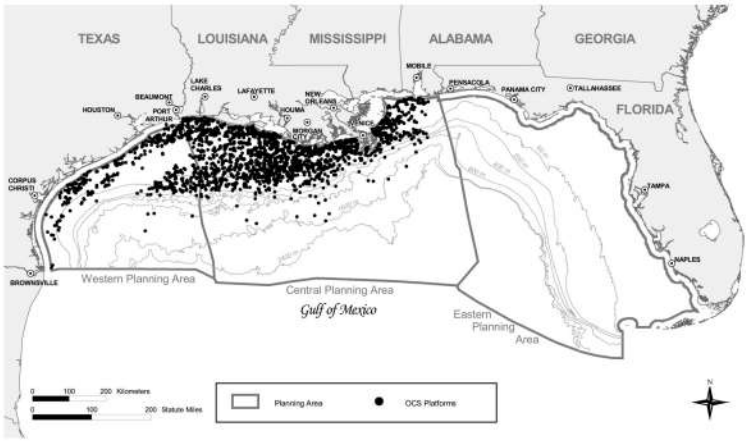

Fig. 2. Planning Areas (Western, Central and Eastern) and platforms for the Gulf of Mexico OCS.

probability for two hindcast time periods that span a total of 13 years, it requires a large amount of computational time. Reducing the number of LPs could reduce the amount of computational time. In this section, a sensitivity study is conducted to evaluate the difference in conditional probability results from using 6,044 LPs versus 3,022 LPs (every other point in Fig. 1)

There are no significant differences between conditional probability at day 30 calculated using 6,044 LPs versus 3,022 LPs. The maximum absolute difference is less than 0.0004 for the annual conditional probability and less than 0.00009 for the monthly conditional probability. However, there are differences in the conditional probability within the first few days of the trajectory launch, which are mainly due to the fact that the LPs are reduced to half of the original number and grid cells directly adjacent to the skipped LPs are not contacted by any trajectories initially.

For the first few days, a checker box pattern is shown on the conditional probability map, resulting from the transformation of a floating point space to an integer space. Note that the OSRA model grid uses the Mercator projection before the trajectories are calculated. After adding a small random noise (0.05º) to both the longitudinal and latitudinal locations of launch points, the edges on the conditional probability map are eliminated. There are no significant differences in conditional probability after a few days between the OSRA model runs without the added noise to the LPs and those with the added noise to the LPs. The OSRA run described in this paper are results from the 3,022 LPs without added noise to the LPs.

C. *Hindcast Surface Winds and Ocean Currents for the 1993–1998 and 2000–2006 Time Periods*

At the time of this study only two GoM ocean model outputs with high temporal resolution of ocean currents (at 3-hourly interval) are available. These data sets are used in the recent OSRA report for lease sales in the Eastern Planning Area of GoM OCS [6]. The hindcast ocean currents were all generated by the Princeton Ocean Model but with different configurations. For the 1993–1998 time period, the winds are 6-hourly, 1ºx1º from European Centre for Medium-Range Weather Forecasts [7]; for the 2000–2006 time period, the winds are 6-hourly, 0.5ºx 0.5º NCEP–QuickSCAT blended [8]. The ocean surface wind data from NCEP–QuickSCAT blended are derived from spatial blending of high-resolution satellite data (SeaWinds instrument on the QuickSCAT satellite) and NCEP reanalysis [9]. The NCEP–QuickScat blended winds were corrected to include the intense wind field during the tropical storms by using high-resolution products from NOAA's Hurricane Research Division. Both models have a large domain that covers the northwest Atlantic Ocean, extending to 55ºW in the east and 50ºN in the north, and also include the Caribbean Sea in the south. The model is initialized using the climatological density, and at the eastern boundary in the Atlantic Ocean, the climatological density and transport are used. It incorporates daily river discharges from 34 rivers. Both models assimilate satellite derived sea surface height and sea surface temperature. For the 1993–1998 time period, an optimal interpolation is used, while a more advanced Ensemble Kalman Filter data assimilation scheme is used for the 2000–2006 time period. For the 2000–2006 run, a nested grid is used in the GoM region with a resolution of 3.5 km; a 5 km resolution is used for the 1993–1998 run.

The model simulations were extensively verified with *in-situ* and satellite-based observations in the GoM [7, 8]. The model is able to reproduce ocean transport and prominent features in the GoM, such as the Loop Current and Loop Current eddies. The model can simulate realistic surface currents both on and off the continental shelf in the GoM.

As mentioned earlier, surface wind data are at 6-hourly interval and ocean currents are at 3-hourly interval for both time periods, and winds and currents are interpolated to an hourly interval to advect the trajectory. To compare these two data sets, monthly climatologies of surface winds and currents are calculated and shown in Figs. 3 and 4 for the 1993–1998 time period and Figs. 5 and 6 for the 2000–2006 time period. Surface winds are primarily northeasterly in the winter, becoming easterly or southeasterly in the summer. During the spring and fall time, the surface winds are mostly easterly or southeasterly. Winds at the West Florida shelf are primarily offshore, where strong northeasterly in winter, easterly in spring, and southeasterly to easterly winds in fall pushes the

particles offshore. The weak onshore winds tend to occur in the summer months.

Surface winds on average are stronger for the 2000–2006 time period compared to the 1993–1998 time period. For example, easterly or southeasterly could exceed 5 m/s in May for the 2000–2006 time period for large portion of the GoM, and winds at the Cayman Island in January, May, July, and November are larger as well. Yet, winds in July are much stronger in offshore Texas and eastern Mexico shelf for the1993–1998 time period while the wind direction remains more or less the same.

The Loop Current and Loop Current eddies are the most energetic features in the GoM circulation. The average Loop Current's eddy-shedding frequency is reported to be 9.5 months, ranging from 3 months to 17 months [10]. Displaying currents on a monthly time scale obviously breaks down the aperiodicity in the eddy-shedding; however, the vulnerability of environmental resources requires the conditional probability to be calculated on a monthly to seasonal basis. Surface currents at the West Florida shelf are weak compared to other areas. Comparison of surface currents between these two periods shows that the Loop Current eddies are slightly stronger for the 2000–2006 time period.

III. Variability of Conditional Probability

A. Interannual Variation of Conditional Probability

The interannual variation of conditional probability is evaluated by estimating the annual conditional probability on a daily basis from day 1 to day 30 for the 1993–1998 and 2000–2006 time periods. There is strong interannual variability in the annual conditional probability at day 30 for the 1993–1998 and 2000–2006 time periods (figures are not shown here), and distinct patterns of conditional probability exist for these two time periods. Areas of highest conditional probability occur near the Loop Current and Loop Current eddies. For the 2000–2006 time period, the conditional probability is very high in the Loop Current eddies. Not surprisingly, the Loop Current area has the highest conditional probability, especially in 1997 and 1998. Another area of relatively high conditional probability for the 1993–1998 time period is at the Texas shelf. A relatively high conditional probability occurs near the Texas shelf at the 20–50 m isobaths in 1994.

The West Florida shelf remains one of the areas with lowest probability of contact despite the fact there are LPs adjacent to it. The low conditional probability in the West Florida shelf agrees with so-called "Forbidden Zone" described in [11], where no drifter ventures to shallow waters off the coast of southwest Florida and Florida Bay (i.e., south of Tampa Bay and west of Florida Bay); it suggests that currents, winds, bathymetry, or all three combined to keep the drifters offshore. The drifters presented in [11] were launched by "Surface Current and Lagrangian-Drift Program (SCULP)" II during February 1996 to June 1997 [12]. Over 300 passive drifters at various locations in the northeastern Gulf, from the Mississippi-Alabama border eastward to off Cedar Key in Florida, were launched, and drifters were tracked via satellite throughout the Gulf and along the Florida Current. While drifters in the SCULP II were deployed mostly north of the Tampa Bay at 28°N, the LPs in this study were located in the "Forbidden Zone" itself, but the trajectories initiated from these LPs were mostly driven away from the shore by the combination effects of currents, winds, and bathymetry.

B. Multi-year Mean and Standard Deviations of Conditional Probabilities

Multi-year mean and standard deviations of annual conditional probabilities for the 1993–1998 and 2000–2006 time periods are calculated every day from day 1 to day 30. Over 1 million trajectories are launched every year for estimating the annual conditional probability as each LP initiates one trajectory every day for a period of 365 days. For the time period of 1993–1998, a total of 6,527,520 trajectories are launched while a total of 7,615,440 trajectories are launched for the time period of 2000–2006. The contacts of these trajectories to each of 20,615 ocean grid cells are tabulated to estimate the multi-year mean annual conditional probability and the standard deviations of annual conditional probability.

Fig. 7 shows the multi-year mean annual conditional probability and standard deviations of conditional probability for the 1993–1998 and 2000–2006 time periods at day 30. The multi-year mean conditional probability at day 30 for these two time periods show a different pattern. For the 2000–2006 time period, the multi-year mean conditional probability reaches a maximum value in the Loop Current eddies and has relatively large values in the Loop Current eddies; for the 1993–1998 time period its counterpart has relatively large value in the Loop Current. For the 1993–1998 time period, the conditional probability is relatively higher, ranging from 0.016 to 0.018, near the Texas shelf. Standard deviations for the conditional probability for both time periods show that the yearly variations reach maximum in the most energetic part of the circulation in the Gulf.

C. Monthly Climatology of Conditional Probability

The monthly climatology of conditional probability is calculated for the periods of 1993–1998 and 2000–2006 at day 30. As shown in Figs. 8 and 9, large seasonal variability exists in the monthly climatology of conditional probability for both time periods at day 30. For the 1993–1998 time period, relatively low conditional probability occurs at the Texas shelf from May to August, and the conditional probability starts to increase during the fall and winter months, as would be expected from the seasonal difference in the Texas–Louisiana coastal circulation [13].

For the 2000–2006 time period, large conditional probability occurs in the anti-cyclonic eddies areas of the GoM in the winter months (i.e., November and January), corresponding to the energetic anti-cyclonic eddies in these months shown in the circulation pattern in Fig. 6. The conditional probability is lowest in May, June, and July. Maximum conditional probability occurs in the anti-cyclonic eddies areas in the western Gulf in the winter months.

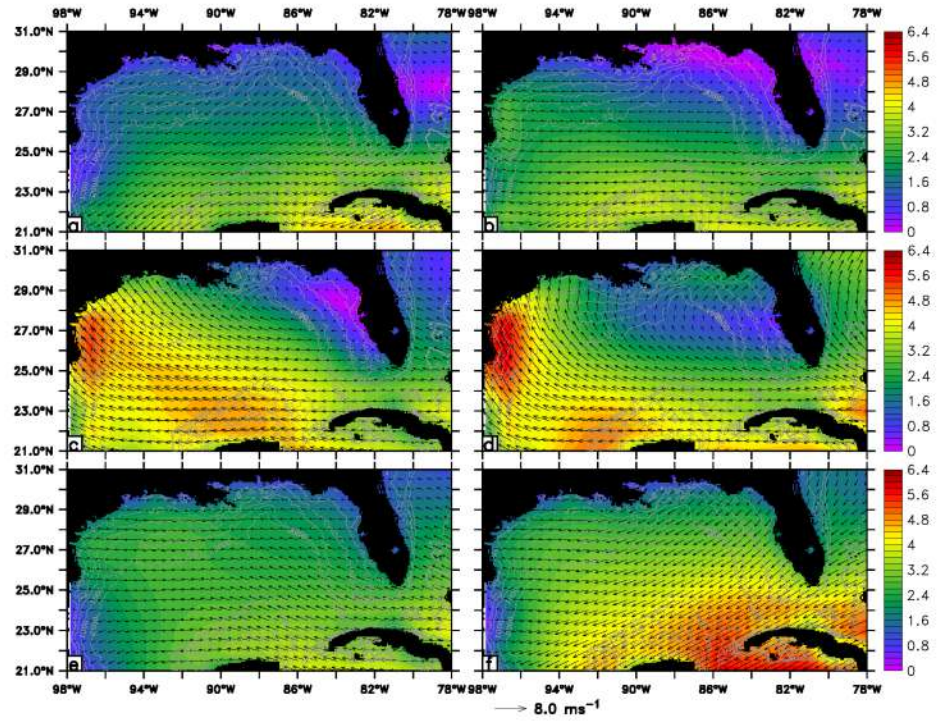

Fig. 3. Monthly climatology of surface wind vector and speed (shaded) from 1993 to 1998: (a) January, (b) March, (c) May, (d) July, (e) September, and (f) November. Units are in m s^{-1}. Isobaths of 20, 50, 200, 1000 and 2000 m are shown as grey lines.

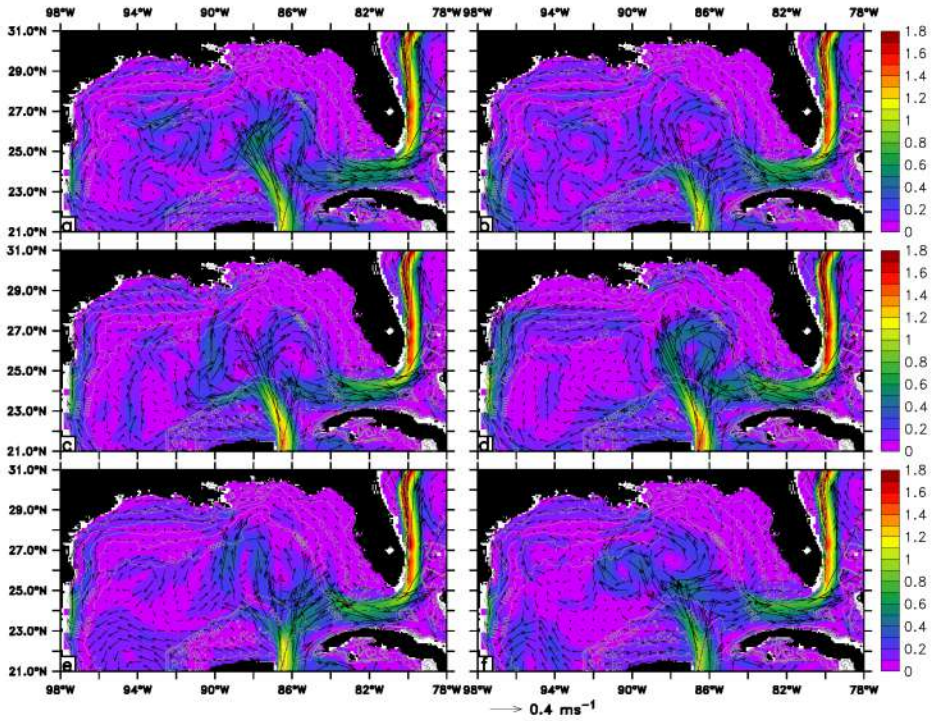

Fig. 4. Monthly climatology of surface current vector and speed (shaded) from 1993 to 1998: (a) January, (b) March, (c) May, (d) July, (e) September, and (f) November. Units are in m s^{-1}. Isobaths of 20, 50, 200, 1000 and 2000 m are shown as grey lines.

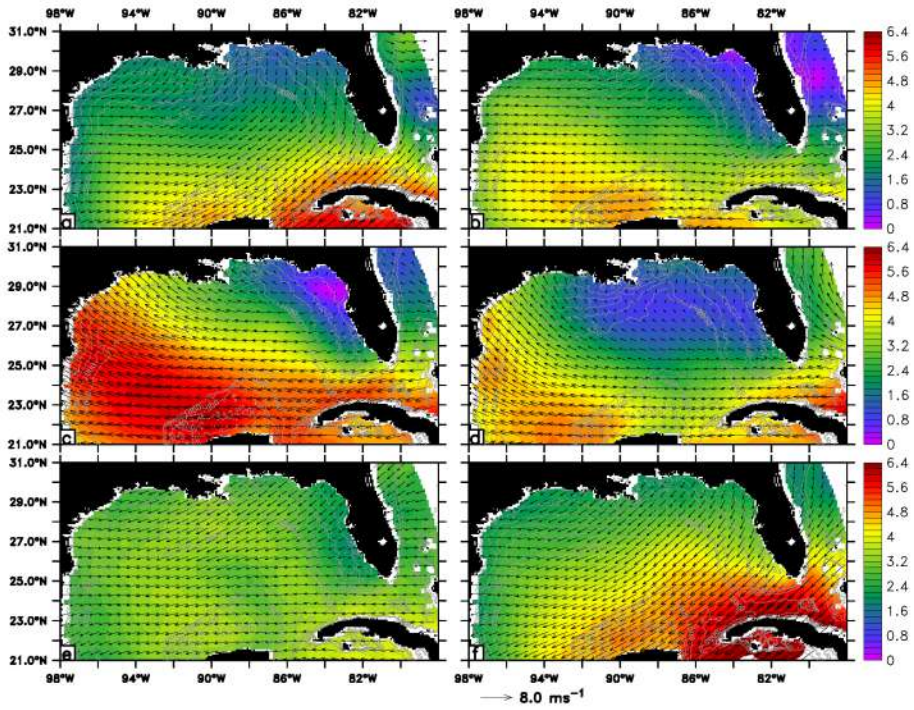

Fig. 5. Monthly climatology of surface wind vector and speed (shaded) from 2000 to 2006: (a) January, (b) March, (c) May, (d) July, (e) September, and (f) November. Units are in m s^{-1}. Isobaths of 20, 50, 200, 1000 and 2000 m are shown as grey lines.

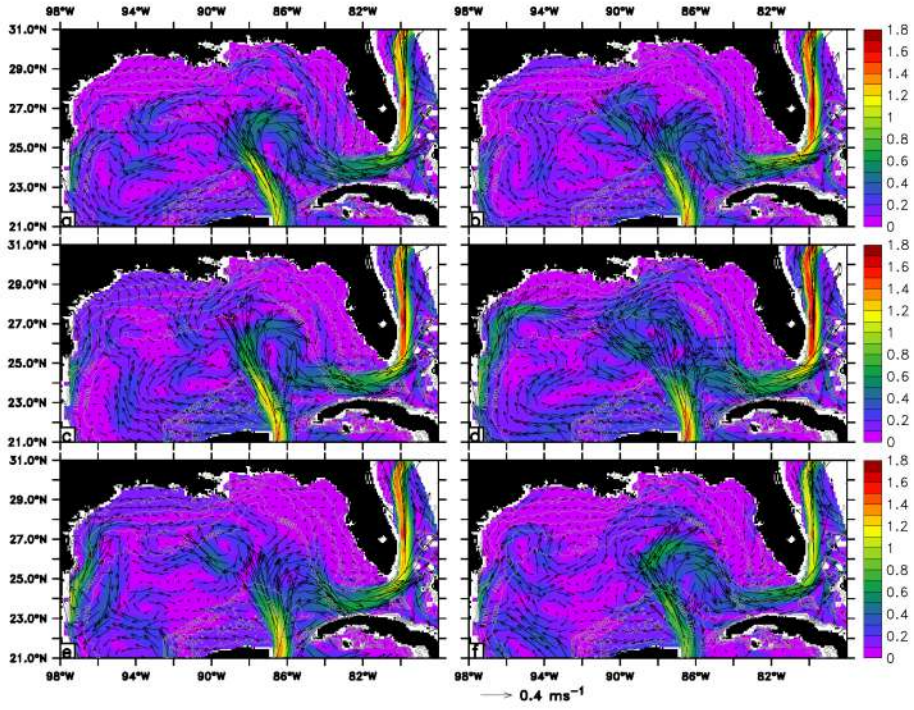

Fig. 6. Monthly climatology of surface current vector and speed (shaded) from 2000 to 2006: (a) January, (b) March, (c) May, (d) July, (e) September, and (f) November. Units are in m s^{-1}. Isobaths of 20, 50, 200, 1000 and 2000 m are shown as grey lines.

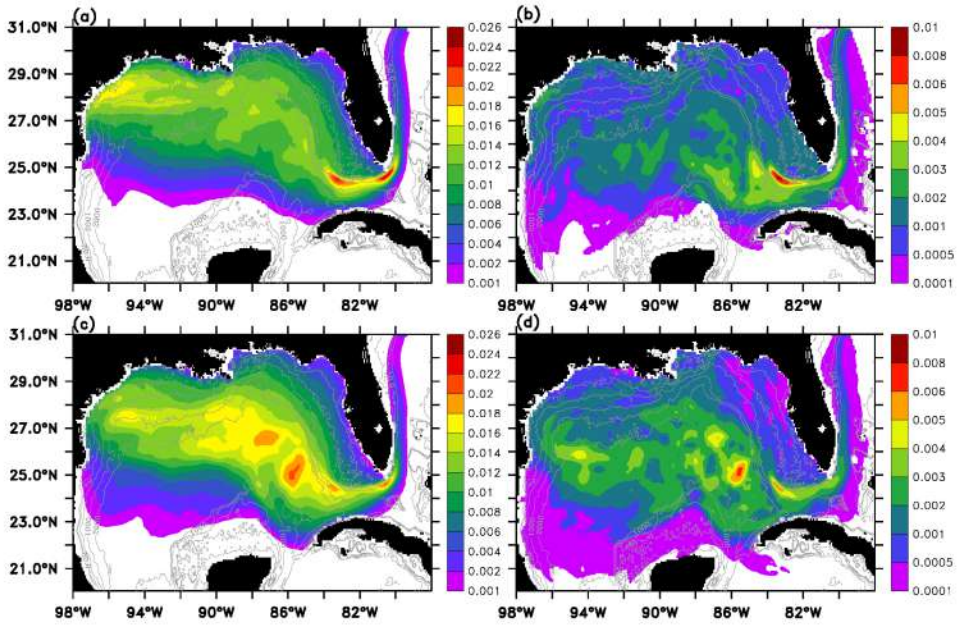

Fig. 7. (a) Multi-year mean of annual conditional probability for 1993–1998 at day 30. (b) Standard deviation of annual conditional probability for 1993–1998 at day 30. (c) Multi-year mean conditional probability for 2000–2006 at day 30. (d) Standard deviation of annual conditional probability for 2000–2006 at day 30.

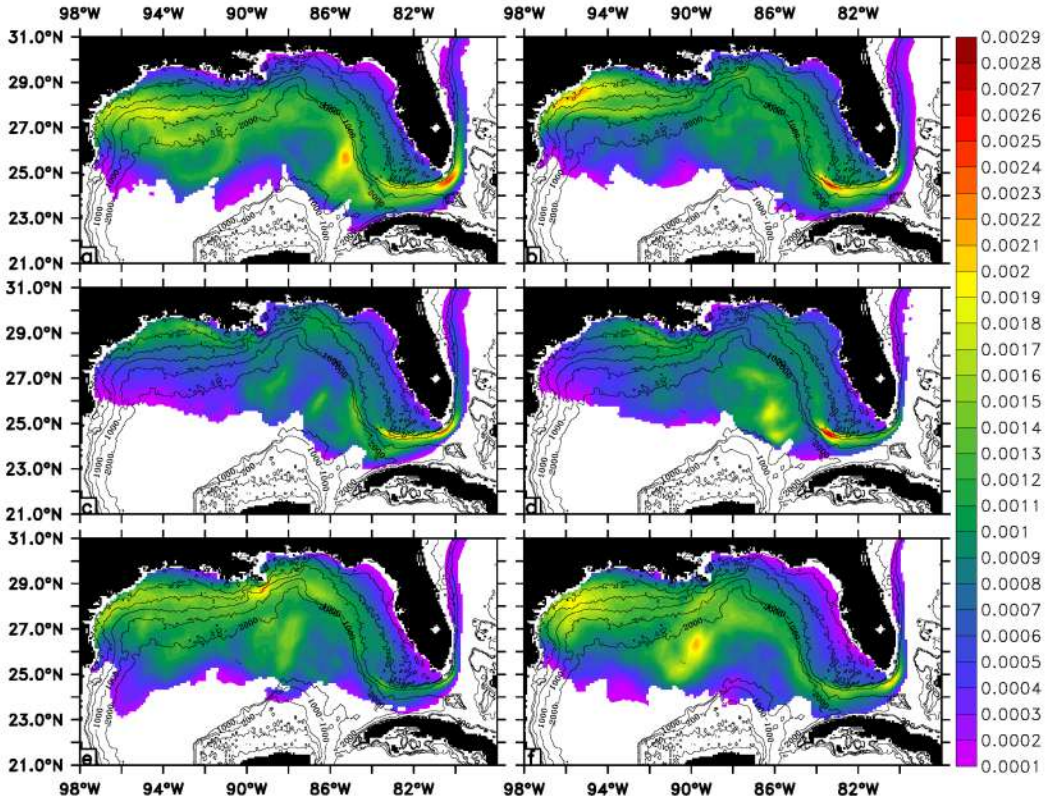

Fig. 8. Monthly climatology of conditional probability at day 30 for the 1993–1998 time period: (a) January; (b) March; (c) May; (d) July; (e) September; (f) November. Isobaths of 20, 50, 200, 1000 and 2000 m are shown as grey lines.

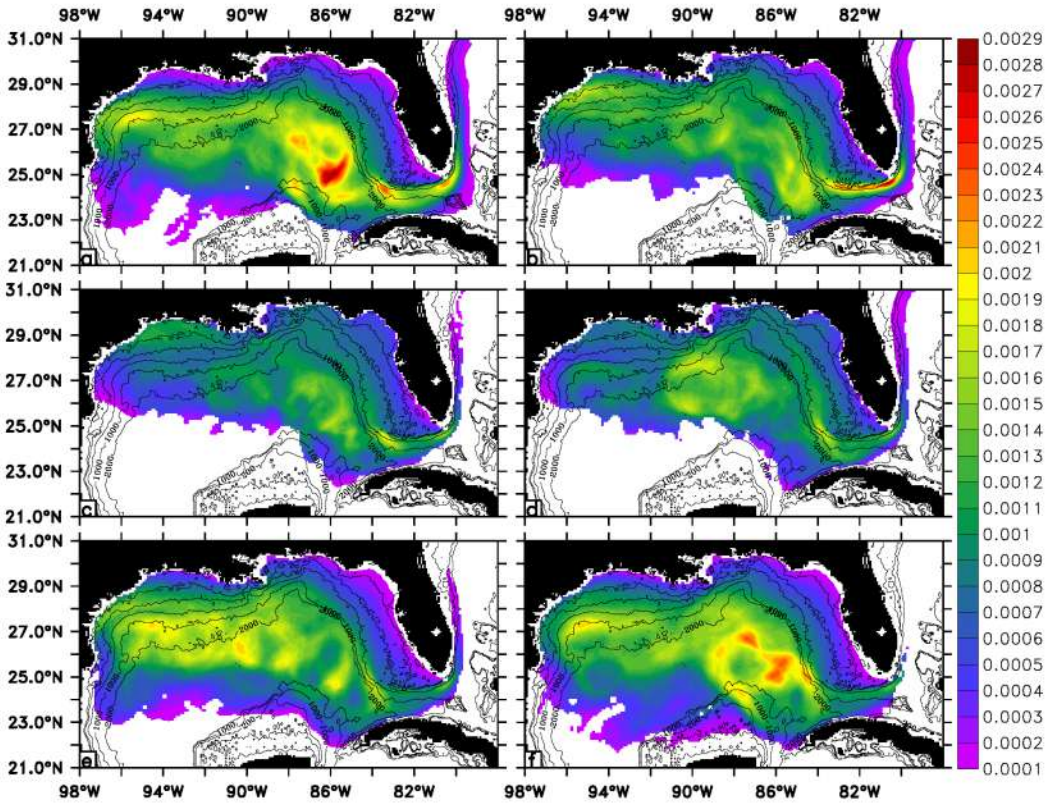

Fig. 9. Monthly climatology of conditional probability at day 30 for the 2000–2006 time period: (a) January; (b) March; (c) May; (d) July; (e) September; (f) November. Isobaths of 20, 50, 200, 1000 and 2000 m are shown as grey lines.

V. Application to an ERA in the GoM

In this section, the new method is applied to estimate the conditional probability of contact to an environmental resource with a seasonally varying location, which demonstrates the advantage of this method. For large environmental resources such as the Sargassum (Fig. 10), a more accurate representation of the conditional probability of contact is to display the histogram of the conditional probabilities within each of these polygons rather than simply using one value to represent the entire polygon.

Fig. 11 shows the conditional probabilities of contact to the Sargassum with a seasonally varying location in the GoM estimated using the surface winds and ocean currents from the time periods of 1993–1998 and 2000–2006. Instead of displaying the total number of grid cells inside the Sargassum that occur within a certain range of the conditional probabilities, the percentages of the grid cells are shown in the vertical axes of the bar charts for three seasonal time intervals and two time periods. There are significant variations of the conditional probabilities within the Sargassum during three different time frames over the two time periods. For March–April, about 40% has a conditional probability of contact around 0.0001 during the time period 1993–1998, while its counterpart has about 30%. For May–June, about 30% of the conditional probability of contact to the Sargassum during the 2000–2006 time period is in the range of 0.0005 while only 5% of its counterpart is in this range. For July–August, the majority of the conditional probability of contact to the Sargassum during the 2000–2006 time period occurs in the range of 0.0015–0.0032 versus that of 0.001–0.0025 for the 1993–1998 time period.

Admittedly, in a real lease sale scenario, each of the proposed leasing area only occupies a small fraction of the GoM OCS, and the LPs are a small subset of the 3,022 hypothetical spill points. However, for a given set of wind and current data, with the number of contacts to each ocean grid cell from all 3,022 LPs archived, the conditional probability from any sets of LPs to any environmental resources with any seasonal vulnerability can be estimated later when needed.

VI. Conclusions and Discussions

A method is developed in this study that can quantify the effects of the wind and surface currents on the statistical distribution of the conditional contact probability. Using this method, the effects of hindcast surface winds and ocean currents from two time periods (1993–1998 and 2000–2006) on the potential oil spill contact probability to entire waters in the GoM are quantitatively evaluated. Results show that strong seasonal and annual variability exists in the distribution of the conditional probability of contact at a given trajectory travel time.

As demonstrated in section 4, the new method makes it possible to accurately estimate and present the contact

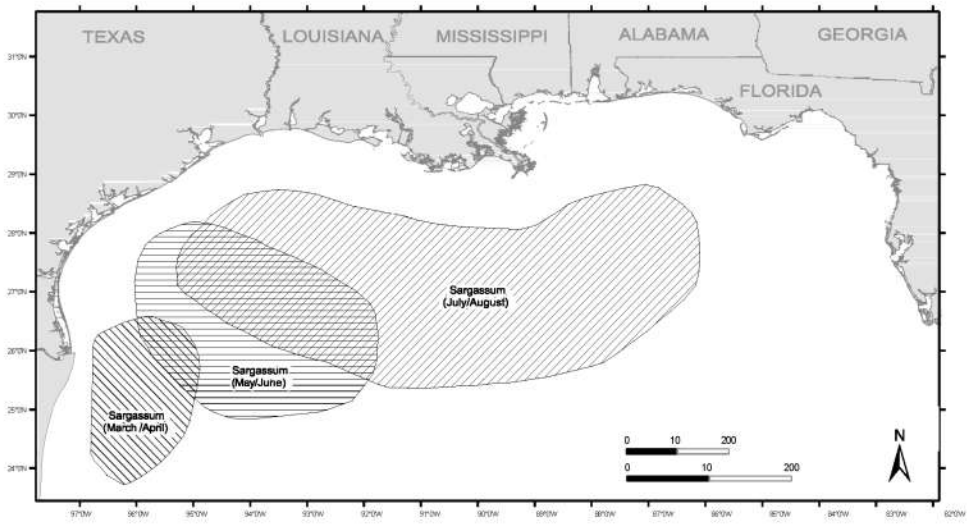

Fig. 10. Locations of Sargassum in the GoM.

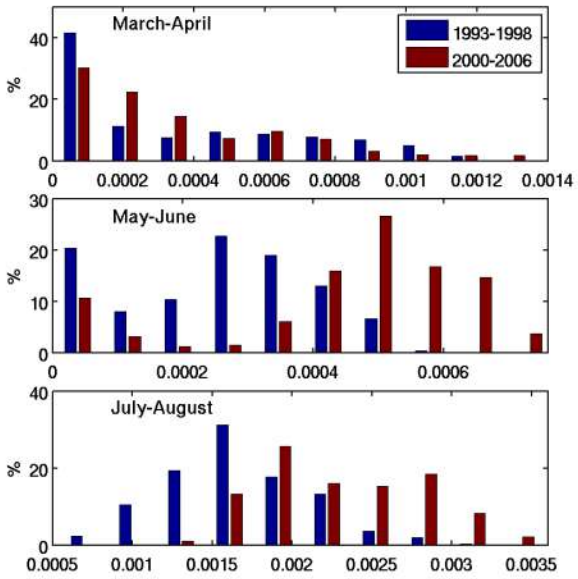

Fig. 11. Conditional probabilities of contact to the Sargassum in the GoM at day 30 displayed as bar charts for March-April, May-June, and July-August for two time periods:1993–1998 (blue) and 2000–2006 (red). The percentages of grid cells inside the Sargassum that occur within a certain range of the conditional probabilities are shown in the vertical axes of the bar charts for three seasonal time intervals and two time periods.

probability for a large and seasonally varying ERA. There are other implications for future spill risk analysis in BOEM, but not limited to the followings:

1) building a geospatial database for the number of contacts to each ocean grid cell from potential oil spill locations for a given set of wind and current data. Should the ERA change, the conditional probability of contact to any ERAs can be calculated from the database without rerunning the OSRA model;
2) estimating the variability in the forcing fields by assigning the standard deviations to the conditional probability;
3) factoring in the density of certain environmental resources, such as a migratory species, when estimating the conditional probability of contact. The density factor can be used to multiply the number of contacts from those OSRA model grid cells that an ERA occupies to get the conditional probability for the ERA.

This study only considers the surface release of hypothetical oil spills without factoring the oil spill volume, weathering, evaporation, emulsification, bio-degradation, and other physical processes that could affect the spill trajectory estimation, such as waves, submeoscale eddies, etc. The OSRA model provides a very conservative estimate of likelihood of oil spill contacts to the ERAs. Additionally, much of the oil released at depth is shown to surface within a few hours and at a radius of a few kilometers [14], so the Monte Carlo approach used in the OSRA model is sufficient to account for the hypothetical oil spill contact to the surface environment resources.

The BOEM aims to improve the OSRA model by reducing uncertainties in the probability of oil spill contacts with environmental resources. BOEM is in the process of acquiring three different sets of hindcast wind and current data from the 2003–2012 time period from different proven ocean models to conduct a multi-model ensemble analysis of OSRA. Using this method, an ensemble of OSRA model solutions can be generated, and uncertainties in the probability of the potential oil spill contacts with the environmental resources in the GoM can be evaluated.

ACKNOWLEDGMENT

We thank Guillermo Auad and Caryn Smith for reviewing our manuscript. The opinions presented here are of authors and do not reflect the viewpoints or policy of the U.S. Government.

REFERENCES

[1] J. M. Price, W. R. Johnson, C. F. Marshall, Z.-G. Ji, and G. B. Rainey, "Overview of the oil spill risk analysis (OSRA) model for environmental impact assessment," Spill Sci. Technol. B., vol. 8, pp. 529–533, 2003.

[2] J. M. Price, W. R. Johnson, C. F. Marshall, Z.-G. Ji, and G. B. Rainey, "Sensitivity testing for improved efficiency of a statistical oil-spill risk analysis model," Environ. Model. Softw., vol. 19, pp. 671–679, 2004.

[3] J. M. Price, et al., "Preliminary Assessment of an Oil-Spill Trajectory Model using Satellite-Tracked, Oil-Spill-Simulating Drifters," Environ. Model. Softw., vol. 21, pp. 258–270, 2006.

[4] Z.-G. Ji, W. R. Johnson, and Z. Li, "Oil spill risk analysis model and its application to the Deepwater Horizon oil spill using historical current and wind data," in Monitoring and Modeling the Deepwater Horizon Oil Spill: A Record-Breaking Enterprise, Y. Liu, A. MacFadyen, Z.-G. Ji, and R. H. Weisberg, Eds. Washington, D.C.: American Geophysical Union, 2011, pp. 227–236.

[5] W. B. Samuels, N. E. Huang, and D. E. Amstutz, "An oil spill trajectory analysis model with a variable wind deflection angle," Ocean Eng., vol. 9, pp. 347–360, 1982.

[6] Z.-G. Ji, et al., "Gulf of Mexico Outer Continental Shelf (OCS) Lease Sales, Eastern Planning Area, 2012–2017, and Eastern Planning Area OCS Program, 2012–2051," BOEM 2013–0110, 2013, 61 pp.

[7] L.-Y. Oey, "Circulation model of the Gulf of Mexico and the Caribbean Sea: Development of the Princeton regional ocean forecast (& hindcast) system – PROFS, and hindcast experiment for 1992–1999," OCS Study MMS 2005–049. Final Report. U.S. Dept. of the Interior, Minerals Management Service, Herndon, Virginia, 2005, 174 pp.

[8] L.-Y. Oey, "Extended hindcast calculation of Gulf of Mexico circulation: model development, comparison with observations, and application to the 2010 oil spill," unpublished.

[9] E. Kalnay, "The NCEP/NCAR 40-year reanalysis project," Bull. Amer. Meteor. Soc., vol. 77, pp. 437–471, 1996.

[10] W. Sturges and R. Leben, "Frequency of ring separations from the Loop Current in the Gulf of Mexico: A revised estimate," J. Phys. Oceanogr., vol. 30, pp. 1814–1819, 2000.

[11] H. Yang, R. H. Weisberg, P. P. Niiler, W. Sturges and W. Johnson, "Lagrangian circulation and forbidden zone on the West Florida Shelf," Continental Shelf Research, vol. 19, pp. 1221–1245, 1999.

[12] W. Sturges, P. P. Niiler and R. H. Weisberg, "Northeastern Gulf of Mexico inner shelf circulation study," Final Report, MMS Cooperative Agreement 14-35-0001-30787. OCS Report MMS 2001 – 103, US Minerals Management Service, Herndon, VA, 90 pp, 2001.

[13] W. D. Nowlin, Jr., A. E. Jochens, S. F. DiMarco, R. O. Reid, and M. K. Howard, "Low-frequency circulation over the texas-louisiana continental shelf," in Circulation in the Gulf of Mexico: Observations and Models, Geophys. Monogr. Ser., vol. 161, W. Sturges and A. Lugo-Fernandez, Eds. AGU, Washington, D. C., 2005, pp. 219–240.

[14] O. Johansen, H. Rye and C. Cooper, "DeepSpill—Field study of a simulated oil and gas blowout in deep water," Spill Sci. Technol. B., vol. 8, pp. 433–443, 2003.